Electronic Journal of Biotechnology 60 (2022) 70–85

Contents lists available at ScienceDirect

Electronic Journal of Biotechnology

journal homepage: www.elsevier.com/locate/ejbt

Research Article

Biochemical, transcriptome and metabolome analysis of the pulp of *Citrus sinensis* (L.) Osbeck 'Hong Jiang' and its two variants reveal pathways regulating pulp taste, mastication, and color

Zhuan-Ying Yang, Xin-Yue Cao, Xue-Wen Zheng, Ting-Qin Wang, Jun-Ning Wang, Feng Feng *, Chun-Hai Ye *

College of Coastal Agricultural Sciences, Guangdong Ocean University, Zhanjiang, Guangdong 524088, China

GRAPHICAL ABSTRACT

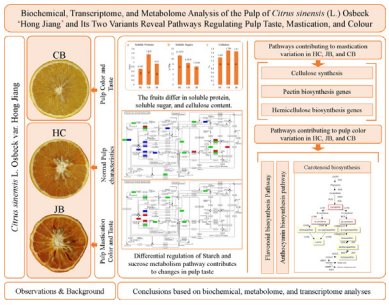

ARTICLE INFO

Article history:
Received 13 February 2022
Accepted 2 September 2022
Available online 13 September 2022

Keywords:
Citrus sinensis
Color
Fruit
Hong Jiang
Mastication
Metabolome
Pulp
Shape
Sweet orange
Taste
Transcriptome

ABSTRACT

Background: Hong Jiang (HC), a grafted chimera of sweet orange (*Citrus sinensis* (L.) Osbeck), is prone to variations in fruit shape, taste, and pulp mastication. We studied the transcriptomes and metabolomes pf pulps of HC and its two variants (CB: fruits with changed pulp mastication, taste, and color and JB: fruits with changed pulp color and taste) to explore the related pathways.
Results: JB accumulated higher organic acids as compared to HC and CB. Flavonoid content was highest in HC followed by JB and CB. The soluble sugar content was lower, while cellulose content was higher in both JB and CB as compared to HC. We found 5,156 and 1,673 DEGs and 283 and 94 DAMs in HC vs JB and HC vs CB, respectively. The differential regulation of starch and sucrose metabolism, galactose metabolism, glycolysis/gluconeogenesis, fructose and mannose metabolism, and citrate cycle pathways could be associated with changes in sugar contents and tastes in JB and CB. Cell-wall polymer-related DEGs/DAMs were associated with the inferior mastication quality of JB and CB. Carotenoid biosynthesis possibly imparts yellowish and reddish pulp color in HC. Additional to this pathway, the anthocyanin biosynthesis led to the changes in JB and CB pulp color.
Conclusions: This combined methodological approach proved to be useful in delineating the large-scale

Abbreviations: DEG, differentially expressed gene; FPKM, fragments per kilobase of exon model per million reads mapped; FDR, false discovery rate; GO, gene ontology; KEGG, Kyoto Encyclopedia of Genes and Genomes; PCA, principal component analysis; qRT-PCR, quantitative real-time PCR; TF, transcription factor.

Peer review under responsibility of Pontificia Universidad Católica de Valparaíso.

* Corresponding authors.
E-mail addresses: ff1703@126.com (F. Feng), gdych@126.com (C.-H. Ye).

https://doi.org/10.1016/j.ejbt.2022.09.001

changes in the transcripts and metabolites of variant fruits in a chimeric citrus variety. This study provides advanced and large-scale data on citrus taste, mastication, and pulp color.

How to cite: Yang Z, Cao X, Zheng X, et al. Biochemical, transcriptome and metabolome analysis of the pulp of *Citrus sinensis* (L.) Osbeck 'Hong Jiang' and its two variants reveal pathways regulating pulp taste, mastication, and color. Electron J Biotechnol 2022;60. https://doi.org/10.1016/j.ejbt.2022.09.001.

1. Introduction

Hong Jiang (HC, *Citrus sinensis* (L.) Osbeck) is a characteristic sweet orange fruit produced in Zhanjiang, Guangdong, China. It is characterized by a relatively large fruit, thin and smooth peel, and has a unique color and balanced sour and sweet taste [1]. For these reasons, HC is preferred by consumers throughout China [2]. From a breeding perspective, HC is a grafted chimeric plant variety and is prone to variations. The variations can lead to changes in fruit taste, color, and appearance [3]. Such variations have been studied in other oranges e.g., Satsuma chimera of 'Zaohong' navel orange and Hongrou Huyou [4,5]. The appearance of chimeras can be spontaneous or artificial and could result in horticulturally beneficial or undesirable changes in fruit esthetics and taste [3,4]. Variations in these chimeras maybe caused by a stable somatic variation in a single cell, which is further transferred to its clonal descendants. This change then persists and can populate a whole meristem leading to the propagation of a new variant [3]. In the case of HC, the types of variations are commonly observed including changes in pulp color, taste, and mastication traits. We observed two types of variations in our experimental area i.e., deformed fruits with changed pulp mastication (abbreviated as JB) and fruits with changed pulp color and taste (abbreviated as CB). We observed that JB and CB fruits sometimes appear on the same HC tree and on the same branch. Preliminary assessment has shown that these fruits have reduced aesthetics and consumer preferences.

Citrus taste/flavor is developed by a complex combination of soluble (organic acids, sugars, and flavonoids) and volatile compounds [6]. Taste, in pulp-containing fruits like citrus, can be a collective outcome of sweetness, bitterness, and sourness. The sweet taste is mainly due to three main carbohydrates i.e., sucrose, fructose, and glucose [7]. The sucrose synthesized in leaves is transported into fruits, where it is converted into fructose and glucose by the action of invertase. However, it may also be broken down into fructose and UDP-glucose. These steps, along with the regulation of the main pathways involved in the biosynthesis of sucrose and its degradation, help the accumulation of carbohydrates upon fruit maturity [8,9]. Other than carbohydrates, naringin and neohesperidine develop bitterness, while citric acid and malic acid are responsible for the sour taste [10]. The ratio of total soluble solids to titratable acids is the main parameter to determine both the quality and the maturity of the citrus fruits. In other words, the ratio of sugars to citric acid content is a good standard for taste considerations [11]. Along with these taste-related traits and respective compounds, the most important quality parameter for the consumers is fruit mastication. Mastication, in juicy fruits like citrus, depends upon the mechanical properties of the pulp. The mechanical properties can be based on the relative content of the cell-wall-related polymers i.e., cellulose, hemicellulose, and pectin. Any visible modification in the pulp could be due to the changes in the texture quality i.e., modification of polysaccharides; increased biosynthesis, solubilization, and/or depolymerization [10,12], whereas, the citrus pulp color is mainly due to two rich pigment families i.e., carotenoids and flavonoids (anthocyanins) [13]. The color of mature fruits varies in different citrus species and depends on the accumulation of different types of carotenoids in the pulp and skin. Most carotenoid biosynthesis genes in citrus are known [14], and hence, the mechanism of color formation in pulp is largely known. Therefore, transcriptomic and metabolomic changes in the chimeric citrus fruits and variants in prouts can help us to understand any changes in pulp color.

Developments in transcriptome and metabolome technologies are enabling us to identify the key genetic and biochemical changes within a chimera and its donors. For example, a recent metabolome profiling of a graft chimera Hongrou Huyou and its two donors (*Citrus changshan-hoyou* and *Citrus unhiu*) enabled the identification of specific metabolites in each donor and the chimera. Similarly, transcriptome profiling of *C. sinensis* helped in the identification of key genes and their expression related to citrate accumulation [15]. Other studies have also explored the transcriptome of *Zanthoxylum bungeanum* Maxim and lemons to identify the genes related to the aroma and high/low acid contents [16]. However, no studies have combined the transcriptome and metabolome data to better understand molecular changes underlying variants. It is essential to understand the key differential transcriptomic signatures and associated metabolic/biochemical changes in such variants. Considering the importance of HC and its consumer preferences, it is essential to understand what types of metabolites are being produced in them and which pathways are being differentially regulated in terms of taste, color, and mastication. In this study, we attempted to understand the key transcriptomic and metabolomic changes in two HC variants having different pulp colors, tastes, and mastication.

2. Materials and methods

2.1. Plant materials and growth conditions

Six-year-old disease- and pest-free Hong Jiang (HC) orange trees bearing normal fruits (HC) and variant fruits i.e., fruits with pulp color and taste variant (JB), and pulp color and mastication variant (CB) were selected. HC is a grafted chimeric citrus variety, which rootstock is *Citrus reticulata* Blanco and the scion is *Citrus sinensis* Osbeck. The trees are growing in the experimental area of Guangdong Ocean University, Zhanjiang, Guangdong, China. In total, we selected nine trees having the normal HC fruits, and variant JB and CB fruits (Fig. 1). Care was taken to select the trees (branches) bearing uniform fruits of each type. Fruits were harvested in September 2020. Three fruits from a tree were selected for each variation characteristic. Fruits were harvested, washed, and photographed followed by the removal of pulp and storage at −80°C before further processing and analyses.

2.2. Biochemical analyses

2.2.1. Determination of organic acids

The contents of the organic acids in the three fruit fleshes were determined by high-performance liquid chromatography (HPLC) following the method described by Liew et al. [17]. Briefly, we weighed 1.0 g of the fruit sample, ground it with 5 mL of 0.2%

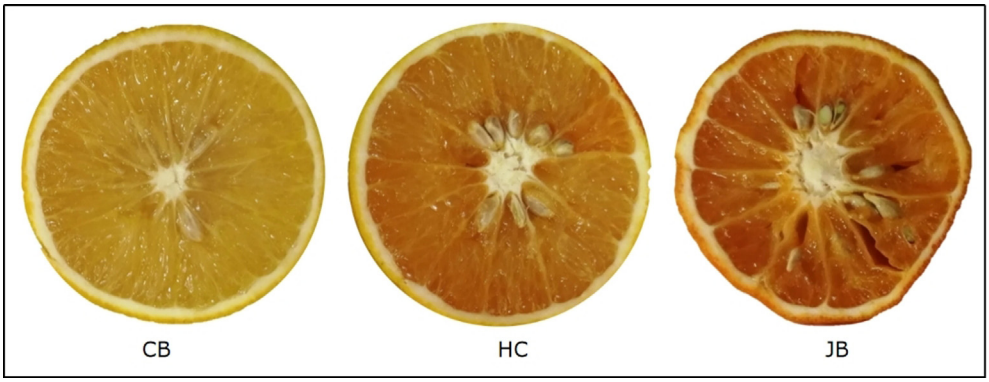

Fig. 1. Hong Jiang (HC) orange fruits with different phenotypes. HC: Hong Jiang (normal); CB: HC with changed pulp color and taste; JB: HC with dark orange color and deformed peel and pulp (changed mastication).

metaphosphoric acid in an ice bath, centrifuged at 10,000 g for 15 min, added 4 mL of 0.2% metaphosphoric acid to the residue and extracted again followed by combining the supernatants, followed by diluting it to 10 mL. After shaking well, 1 mL was taken, filtered through a 0.45 μm filter membrane, and put it into a liquid phase injection for analysis. HPLC was used to determine the organic acid components of fruits. Column: eclipse plus C18 (5 μm, 4.6 × 250 mm); mobile phase: 0.2% metaphosphoric acid solution, flow rate 1.0 mL/min; injection volume 10 μL; column temperature 35°C; UV detection wavelength 210 nm.

2.2.2. Determination of flavonoid contents

We weighed 1.0 g of the fruit sample, added 10 mL methanol as the extraction solvent, and heated it in a 30°C water bath for 1 h for the determination of flavonoid contents. The solution was filtered, the extraction was repeated with 10 mL methanol once, and the two extracts were combined. After shaking well, 1 mL was taken and filtered through a 0.45 μm filter membrane and used for HPLC analysis: column: eclipse plus C18 (5 μm, 4.6 × 250 mm); mobile phase: acetonitrile-0.5% acetic acid solution (20:80 by volume), flow rate 1.0 mL/min; injection volume 10 μL; column temperature 40°C; UV detection wavelength 283 nm.

2.2.3. Determination of soluble proteins, sugars, and cellulose content

The soluble protein content in the three types of fruits was determined by the Coomassie brilliant blue G-250 colorimetry method [18]. Soluble sugar content and cellulose content were determined by following an improved calorimetric method as reported in [17,19].

Microsoft Excel 2013 was used for data sorting, and SPSS statistical software was used for statistical analysis.

2.3. Transcriptome analyses

All the transcriptome analyses were performed at Wuhan Metware Biotechnology Co., Ltd, Wuhan 430070, China. Brief descriptions of the methods are given below.

2.3.1. RNA extraction

Total RNAs were extracted from the pulps of the three fruits for each technical replicate i.e., HC, JB, and CB as reported earlier [20]. Following RNAs' extraction, their integrity was tested and they were quantified using agarose gel electrophoresis, 2100 Agilent Bioanalyzer, and a Qubit 2.0 Fluorometer.

2.3.2. Library preparation and sequencing

The cDNAs from each extracted and quantified RNA were extracted, libraries were prepared, and quantified using a Qubit 2.0 Fluorometer. We then accurately determined the concentrations of the libraries using the Q-PCR method. The libraries with an effective concentration of >2 nM were pooled for each biological replicate and sequenced on the Illumina HiSeq platform.

2.3.3. Data analyses

Raw reads were processed for the removal of the low-quality reads (if bases with $Q \leq 20$ exceeded 50% of the bases contained in the sequencing reads) using FastQC. Furthermore, we also checked the GC content distribution and obtained clean reads of subsequent analyses. We then used HISAT2 [21] to compare the clean reads with the reference genome and determined the comparison efficiency.

2.3.4. Gene expression quantification

The Fragments Per Kilobase of transcript per Million fragments mapped (FPKM) was used as an index to measure the expression level of transcripts. The FPKM values were then used to visualize the overall distribution of the gene expression, measure Pearson Correlation Coefficient (PCC), and Principal Component Analysis (PCA) in karyoplotR [22]. Differentially expressed genes (DEGs) were identified using feature Counts [23], and the Benjamini-Hochberg method [24] was used to calculate P values for measuring the false discovery rate (FDR). The transcripts/genes with log2 foldchange (log2 FC) value of ≥ 1 and ≤ -1 and FDR < 0.05 were considered as DEGs and MA plots, heatmaps, and Venn diagrams were generated [25].

2.3.5. Functional annotation of DEGs and pathway enrichment

The DEGs were then functionally annotated in KEGG, GO, and KOG databases as reported in an earlier study [26]. The DEGs were then enriched on different KEGG pathways based on Rich factor, Q value, and the number of genes in each pathway.

2.4. qRT-PCR analysis

To validate the RNA sequencing results, 14 genes were selected to perform qRT-PCR analyses. Primers were designed in the Primer3 tool (Table 1). The PCR setup and reaction conditions were as reported earlier [20]. The relative gene expression was computed with the *Actin* gene as an internal control [20]. Each qRT-PCR reaction was conducted with three biological replicates and technical replicates.

Table 1
List of primers used for qRT-PCR analyses of the selected genes.

Gene ID	Forward primer sequence	Reverse primer sequence
Cs5g11560	TGCAACCAAGGCATCA	TGCACTGTCGGCTTT
Cs9g18700	CCAGGTGCGTTGA	CACTGTCTCTGGGCT
Cs1g18220	TCAGGAAGATTGCTGC	CAAACCATCCTGACTC
Cs3g03130	GATGGATGACTAGT	ATTAATCGAATCCTT
Cs6g16770	GCTTCCGGTTATGG	CCAGCTCTGCTTAAT
orange1.1t00636	CGCCTTTCTCTATCC	CATTCAGGTCCACT
Cs9g14600	ACTGCACCCTCTGC	GCACGTGACCTTTA
Cs1g15970	TCAAAGTGTAGCGATC	TCTTTTTGTTTATG
Cs2g12290	CAAACGCATATCAATC	AGCAACGCGACATTG
Cs1g20920	GGTGAGTCGGGAGT	TCCATGCAACGAA
Cs4g13070	GTCTCGATCACCT	TTCCCATCATTAGCCC
Cs6g08840	GCCATTCATTTGGTGC	GCATTCACCCCGTAATA
Cs9g03400	TGGACAAATCACACA	TTGAATCCATCATAG
Cs1g18240	CTGATGCACTATGCG	ACCGCACTGTTCAAT
Actin	TGGTTCATACATCCGG	CATAATTGATGCCTCC

2.5. Metabolome analyses

2.5.1. Extraction

The freeze-dried pulp of three replicates of each fruit type (HC, JB, and CB) were crushed to powder in a Retsch MM 400 mixer mill. A total of 100 mg powder was extracted overnight in 0.6 ml (70% MeOH) at 4°C. Centrifugation of the extract was done at 10,000 g for 10 min, and the extracts were further used for UPLC-MS/MS analysis after they were absorbed (CNWBOND Carbon-GCB SPE Cartridge, 250 mg, 3 ml; ANPEL, Shanghai, China, www.anpel.com.cn/cnw) and filtrated (SCAA-104, 0.22 μm pore size; ANPEL, Shanghai, China, http://www.anpel.com.cn/).

2.5.2. UPLC conditions and ESI-Q TRAP-MS/MS

Triplicate extracts of each fruit type were analyzed in UPLC-ESI-MS/MS system (UPLC, Shim-pack UFLC SHIMADZU CBM30A system, www.shimadzu.com.cn/; MS, Applied Biosystems 4500 Q TRAP, www.appliedbiosystems.com.cn/). The analytical conditions, LIT, and triple quadrupole (QQQ) scan acquirement were done at Wuhan Metware Biotechnology Co., Ltd, Wuhan 430070, China as reported earlier [20].

2.5.3. Data analyses

The unsupervised PCA, hierarchical cluster analysis, and PCC were completed in R (www.r-project.org) using prcomp, cor function, and pheatmap, respectively.

Differentially accumulated metabolites (DAMs) between the different types of fruits were determined by VIP (variable importance in projection) $\geq$ 1 and log2 FC $\geq$ 1 and $\leq$ -1. We used MetaboAnalystR for the calculation of VIP scores to the OPLS-DA model [27]. The identified metabolites were annotated using the KEGG compound database (http://www.kegg.jp/kegg/compound/) and mapped on KEGG pathways and significantly regulated ones were determined based on the hypergeometric test's p-values.

2.6. Joint data analysis of transcriptome sequencing and metabolite profiling results

The identified DEGs and DAMs were jointly mapped on KEGG pathways [28], and significantly regulated pathways were identified and a combined histogram was generated. PCC between DEGs and DAMs was computed in R (cor) and represented as a nine-quadrant heatmap [29].

Table 2
Composition and content of organic acid in the fruits of the three *C. sinensis* varieties.

Fruit type	Malic acid (mg/g)	Citric acid mg/g)	Ascorbic acid (mg/g)
JB	1.288 ± 0.007 cB	14.399 ± 0.189 aA	0.311 ± 0.005 aA
HC	1.451 ± 0.048 aA	7.071 ± 0.328 bB	0.233 ± 0.006 cB
CB	1.359 ± 0.010 bB	4.150 ± 0.028 cC	0.301 ± 0.001 bA

Note: The values represent means of the three replicates. Lowercase letters in the same column indicate significant differences between varieties ($P < 0.05$), and uppercase letters indicate significant differences between organic acids ($P < 0.01$). The numbers after ± are standard deviations.

3. Results

3.1. Biochemical analysis

The organic acid content analysis showed that the highest content in the three types of fruits was citric acid followed by malic acid and ascorbic acid (Table 2). Among the three varieties, the highest citric acid content was found in JB followed by HC and CB. The highest malic acid content was present in HC, and it was significantly different from that of JB and CB, whereas, the highest ascorbic acid content was present in JB followed by CB and HC (Table 2).

Flavonoid content analyses in the three fruit types indicated the absence of hesperidin; however, neohesperidin and naringin were detected. Neohesperidin was the main flavonoid in all three varieties. The naringin content differed significantly in the three fruit types. HC had the highest content followed by CB and JB. On the contrary, JB had the highest neohesperidin content followed by HC and CB (Table 3).

A significantly high level of soluble protein content was present in CB, followed by HC and JB (no significant differences) (Fig. 2a). Regarding soluble sugars, HC had significantly higher content followed by CB and JB (Fig. 2b). CB and JB had similar cellulose content which was significantly higher than HC (Fig. 2c).

3.2. Transcriptome sequencing of pulp of HC, JB, and CB fruits

Sequencing of nine cDNA libraries with Illumina Hiseq platform resulted in 61.94 Gb clean data. The error rate, Q20 base %, Q30 base %, and GC content % were 0.02%, > 98%, > 94%, and > 43.96%, respectively. More than 90% of the reads could be mapped with > 87% reads that were uniquely mapped to the reference genome (Table S1). Overall, FPKM for JB and CB was higher than HC (Fig. 3a). The PCC between the replicates of the three treatments was >0.97, indicating the reliability of the results (Fig. 3b). Similarly, the PCA plot showed that replicates of each pulp type were grouped. PC1 explained 43.51% and PC2 explained 20.14% variability (Fig. 3c). These results suggest that significant differences exist in gene expression profiles of HC, JB, and CB.

3.2.1. Differential gene expression and KEGG pathway enrichment

Based on the screening criteria i.e., log2 FC $\geq$ 1 and $\leq$ -1 and FDR < 0.05, 5,156, 1,673, and 5,052 genes were differentially

Table 3
Composition and content of flavonoids in the fruits of the three *C. sinensis* varieties.

Fruit type	Naringin content (mg/g)	Neohesperidin content (mg/g)
JB	0.149 ± 0.001 cC	2.665 ± 0.002 aA
HC	0.454 ± 0.003 aA	2.513 ± 0.006 bB
CB	0.263 ± 0.009 bB	2.128 ± 0.046 cC

Note: Lowercase letters in the same column indicate significant differences between varieties ($P < 0.05$), and uppercase letters indicate significant differences between flavonoids ($P < 0.01$).

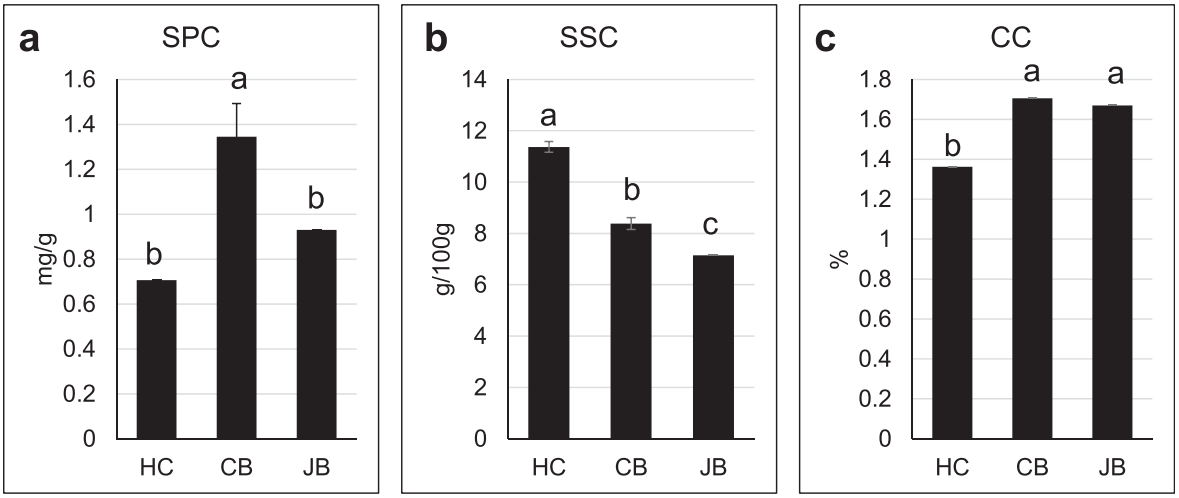

Fig. 2. (a) Soluble protein (SPC), (b) Soluble sugar (SSC), and (c) Cellulose content (CC) in the three fruit types. The graphs represent mean values of three replicates. The error bars represent standard deviation.

expressed in HC vs JB, HC vs CB, and CB vs JB, respectively (Fig. 4a). To verify the gene expression profile from the RNA-seq, we selected 14 differentially expressed genes (DEGs) and performed qRT-PCR analysis. The results showed differential expression patterns of the selected genes between HC, JB and CB, confirming the reliability of our DEG analysis (Fig. S1).

Biosynthesis of secondary metabolites (KO01110), phenylpropanoid biosynthesis (KO00940), metabolic pathways (KO01100), MAPK-signaling pathway (KO04016), plant-pathogen interaction (KO04626), plant hormone signal transduction (KO04075), flavonoid biosynthesis (KO00941), glycolysis/gluconeogenesis (KO00010), and glutathione metabolism (KO00480) were the pathways in which DEGs were significantly enriched between HC and JB (Fig. 4b). In the treatment comparison HC vs CB, the top five pathways in which the DEGs were enriched included metabolic pathways (KO01100), biosynthesis of secondary metabolites (KO01110), phenylpropanoid biosynthesis (KO00940), α-linolenic acid metabolism (KO00592), and MAPK signaling pathway (KO04016) (Fig. 4c). Between JB and CB, the top five pathways in which DEGs were significantly enriched were metabolic pathways (KO01100), biosynthesis of secondary metabolites (KO01110), phenylpropanoid biosynthesis (KO00940), flavonoid biosynthesis (KO00941), and glycosphingolipid biosynthesis (KO00604) (Fig. 4d).

3.2.2. Differential gene expression in sugar-related pathways

3.2.2.1. HC vs JB. Three pathways i.e., fructose and mannose metabolism, amino sugar and nucleotide sugar metabolism, and starch and sucrose metabolism were significantly enriched between HC and JB. There were 19, 35, and 58 DEGs enriched in these pathways, respectively. Ten of the 19 DEGs enriched in fructose and mannose metabolism were downregulated in JB as compared to HC; two 6-phosphofructokinase 1 s, two diphosphate-dependent phosphofructokinases, one fructokinase, one fructose-bisphosphate I, three fructose-bisphosphate aldolases, one hexokinase, and one mannan endo-1,4-β-mannosidase (Fig. S2a). Four of the five fructokinases were upregulated in JB as compared to HC suggesting the breakdown of D-fructose into β-D-fructose 6P, which further takes part in glycolysis. Another gene that controls an important step in this pathway i.e., conversion of 1,4-β-mannan to D-mannose, was differentially regulated between JB and HC. This step also leads to the breakdown of D-fructose into β-D-fructose 6P. The downregulation of fructose-bisphosphate aldolases suggests that in JB, the degradation of β-D-fructose 6P into glyceraldehyde-3P and/or the interconversion of D-fructose 1P and glycerone-P was reduced. This step is central and connects sugar and organic acid metabolism. Overall, these transcriptional changes suggest that HC has higher D-fructose levels and in JB, it is being differentially regulated. Additionally, we found four sucrose synthases (SUS, *Cs4g06850, Cs4g06900, Cs6g15930*, and *Cs9g03980*) in our transcriptome results. Three of these (except *Cs6g15930*) were downregulated in JB as compared to HC indicating that in JB, sucrose synthesis was reduced. These expression changes are consistent with the observation that HC had higher soluble sugar content than JB.

The biosynthesis of amino sugars i.e., N-Acetylchitosamine (GlcNAc) from chitin was increased as evident from the upregulation of hexosaminidase. However, further degradation of GlcNAc into UDP sugars is reduced. We say this since we observed the downregulation of genes such as hexokinases, glucosamine-fructose-6-phosphate aminotransferase, cytochrome-b5 reductase, reversibly glycosylated polypeptide/UDP-arabinopyranose mutase, α-N-arabinofuranosidase, and UDP-glucose 6-dehydrogenase in JB as compared to HC (Fig. S2b).

Transcripts of most of the DEGs that were enriched in starch and sucrose metabolism were both up- and downregulated at the same time. The major downregulated genes in JB as compared to HC were β-fructofuranosidases (6 genes), trehalose 6-phosphate synthase/phosphatase (2 genes), ectonucleotide pyrophosphatase/phosphodiesterase family members (2 genes), glucose-1-phosphate adenylyltransferase (2 genes), β-amylase (2 genes), and a hexokinase. These expression changes between HC and JB suggest that the arriving sucrose-6P in HCs pulp is being converted into D-fructose (and D-fructose 6P), and D-glucose. While in the case of JB (as compared to HC), multiple genes are being up/downregulated at the same time that are involved in amylose, maltodextrin, maltose, and dextrin synthesis (Fig. 5a).

Other sugar-related pathways in which the DEGs were enriched between HC and JB included galactose metabolism (24 DEGs) and glycolysis/gluconeogenesis (39 DEGs). Genes (β-galactosidase and hexokinase) controlling the conversion of α-D-glucose, and galactose had reduced expression in JB as compared to HC. The expression of three genes (raffinose synthase, stachyose synthetase, and α -glucosidase) that are involved in the synthesis of raffinose, stachyose, and D-fructose had increased expression in JB as compared to HC, while multiple α-galactosidases were variably regulated between both fruit types. These expression changes indicated that in JB, the synthe-

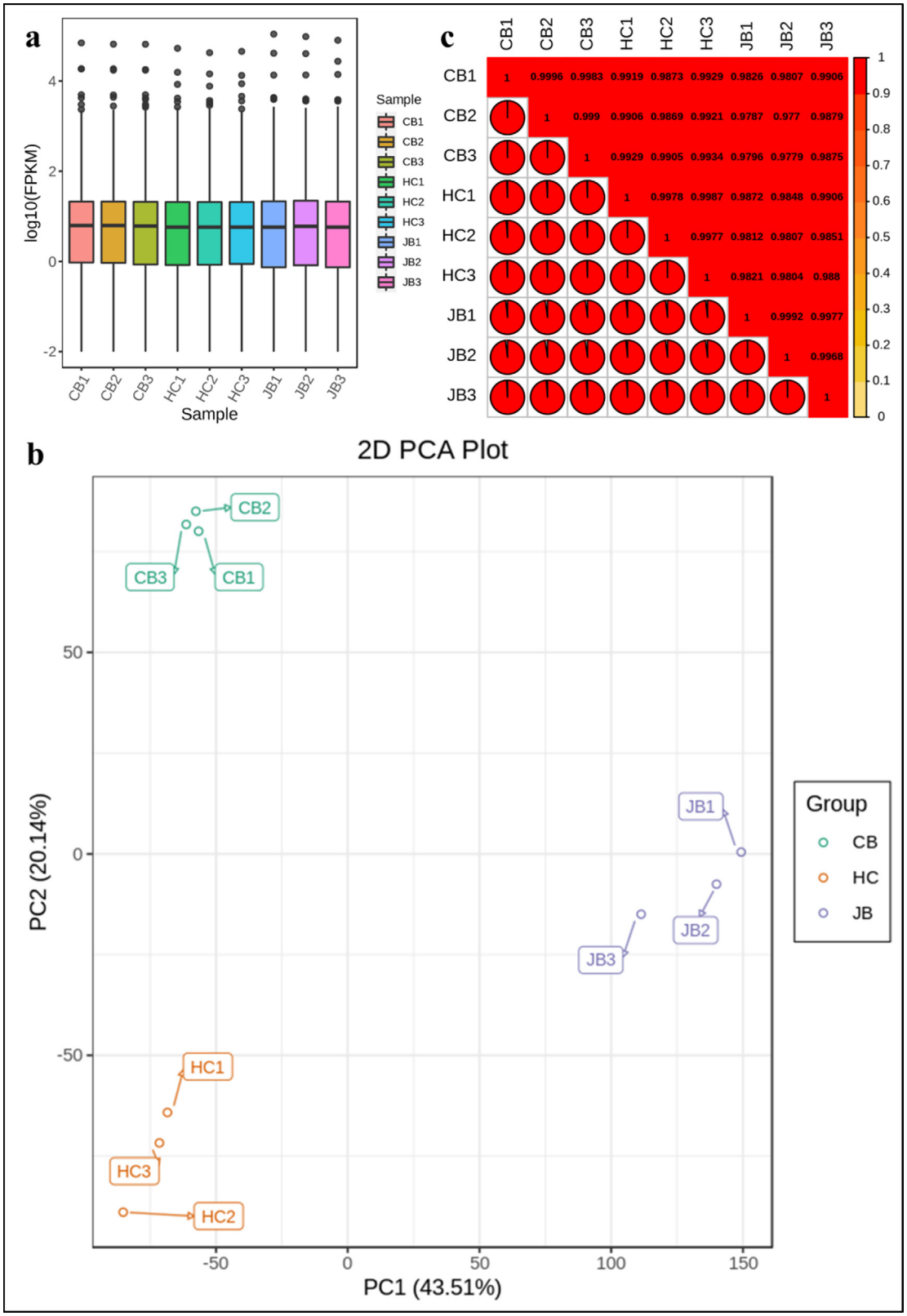

Fig. 3. (a) Distribution of the gene expression (log_{10}(FPKM)), (b) principal component analysis, and (c) Pearson Correlation Coefficients between replicates of HC, JB, and CB.

sis of D-galactose, and D-glucose was reduced and/or varied, while the synthesis of D-fructose from galactinol increased as compared to HC. Only two genes annotated as phosphoenolpyruvate carboxykinase (ATP) and glucose-6-phosphate 1-epimerase were upregulated in JB as compared to HC. All other DEGs were either downregulated or expressed variedly. These downregulated genes were enriched in most of the intermediate steps of interconversions of β-D-fructose 6P and acetyl-CoA.

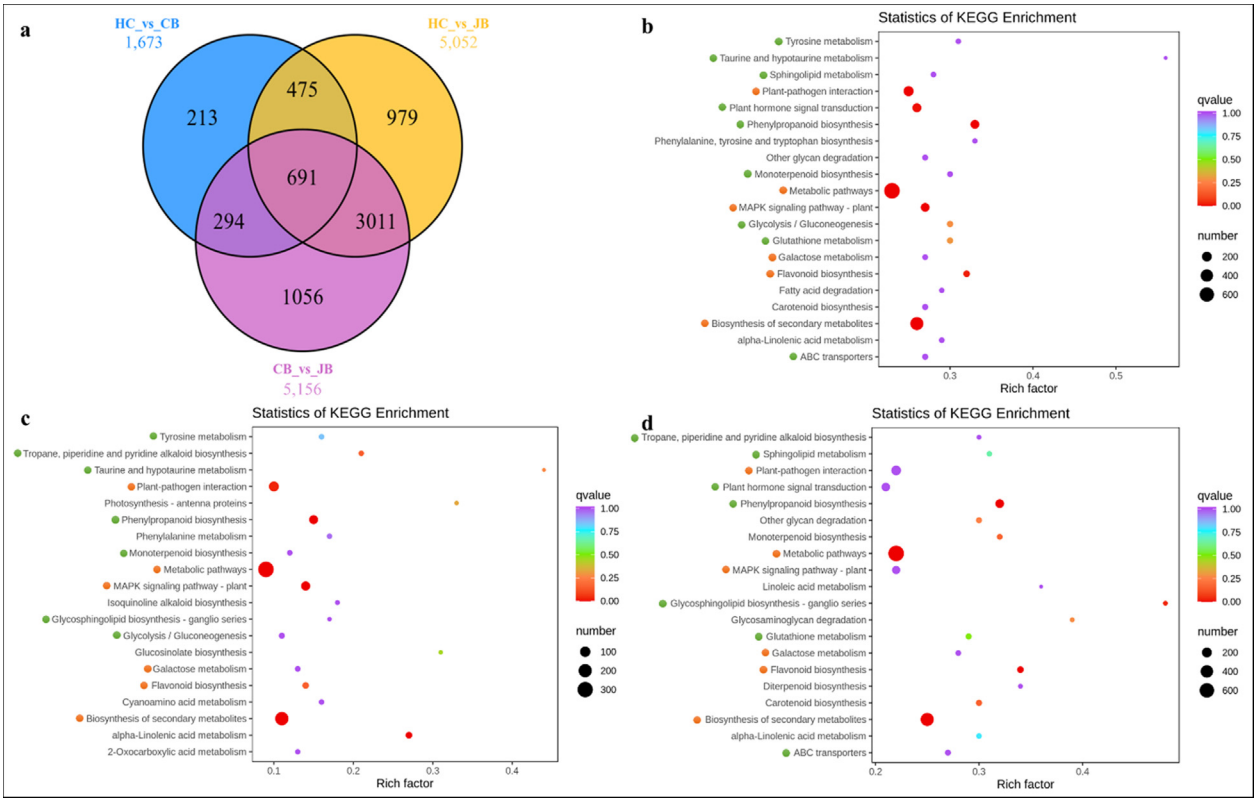

Fig. 4. (a) Venn diagram of DEGs and significantly enriched pathways in treatment comparisons (b) HC vs JB, (c) HC vs CB, and (d) CB vs JB. The orange and green dots with the pathway names show that the pathway is common between three and two treatment comparisons, respectively.

3.2.2.2. HC vs CB. Only five DEGs belonging to the fructose and mannose metabolism pathway were differentially expressed between HC and CB. Two 6-phosphofructokinase 1 s and a diphosphate-dependent phosphofructokinase were downregulated and two mannan endo-1,4-β-mannosidases were upregulated in CB as compared to HC. Their expression patterns suggest that in CB, the β-D-fructose 6P conversion into β-D-fructose 1-6P_2 was reduced, while the conversion of 1,4-β-mannan to D-mannose increased as compared to HC (Fig. S2c).

The expression changes in the CB pulp as compared to HC pulp indicated similar changes as observed in JB vs HC pulp. However, a relatively lower number of genes enriched in sucrose and starch metabolism were differentially expressed between HC and CB. Two SUSs (*Cs4g06850* and *Cs6g15930*) were downregulated in CB as compared to HC. In any case, the expression changes indicate that sucrose biosynthesis and its conversion into trehalose, D-fructose, and D-glucose were reduced (Fig. 5b). These expression changes correspond with the observed lower soluble sugar contents in CB as compared to HC (Fig. 2b).

A relatively lower number of genes (12) related to galactose metabolism were differentially expressed between HC and CB as compared to the comparison between HC and JB i.e., 24. Interestingly, we observed that genes that synthesize D-galactose and D-glucose were upregulated in CB as compared to HC. Furthermore, the synthesis of sucrose from raffinose (by the action of α-galactosidase) was increased in CB as compared to HC due to the increased expression of *Cs5g17230*. On the other hand, the gene (*Cs2g10900*) controlling D-fructose biosynthesis from raffinose (where sucrose is intermediate) was not differentially expressed between HC and CB. This gene was upregulated in JB as compared to HC. Hence, most probably, this step is different between the three pulp types.

Only 15 genes enriched in the glycolysis/gluconeogenesis pathway were differentially expressed between HC and CB. Only one gene (acetate-CoA ligase; *Cs9g02540*) was upregulated in CB, while all other genes enriched in this pathway had reduced expressions in CB as compared to HC. It can be stated that the conversion of the oxaloacetate (from citrate cycle) to phosphoenolpyruvate was reduced due to the decreased expression of phosphoenolpyruvate carboxykinase (ATP) (*Cs9g20920*) in CB as compared to HC, while in the case of JB, the expression was increased (Table S2).

3.2.3. Differential regulation of genes related to bitterness and sourness

3.2.3.1. HC vs JB. A major compound that causes (immediate) bitterness is naringenin [30]. Naringenin is synthesized by the flavonoid biosynthesis pathway; which was one of the pathways in which the DEGs were significantly enriched. Forty-five DEGs were enriched in the flavonoid biosynthesis pathway between HC and JB. Twenty-four of the DEGs were shikimate O-hydroxycinnamoyltransferase; ten of which were upregulated and 14 were downregulated. We observed the downregulation of two important genes i.e., trans-cinnamate 4-monooxygenase (*Cs4g04530*) and chalcone synthase (*Cs3g19360, Cs3g20330, Cs3g20680, Cs9g11190,* and *orange1.1t05430*) in JB as compared to HC. These genes successively convert cinnamoyl-coA into p-coumaroyl-coA and then into naringenin chalcone. These transcriptional changes suggested that naringin biosynthesis is being affected at least at these two steps. However, the other genes which take part in the conversion of naringenin chalcone into naringin were not differentially expressed between HC and CB. On the other hand, we observed that the expression of the genes that control the final steps of the biosynthesis of phlorizin (i.e., phlorizin synthase; *Cs9g18820* and *Cs9g18830*), (+)-afzelechin, (+)-catechin,

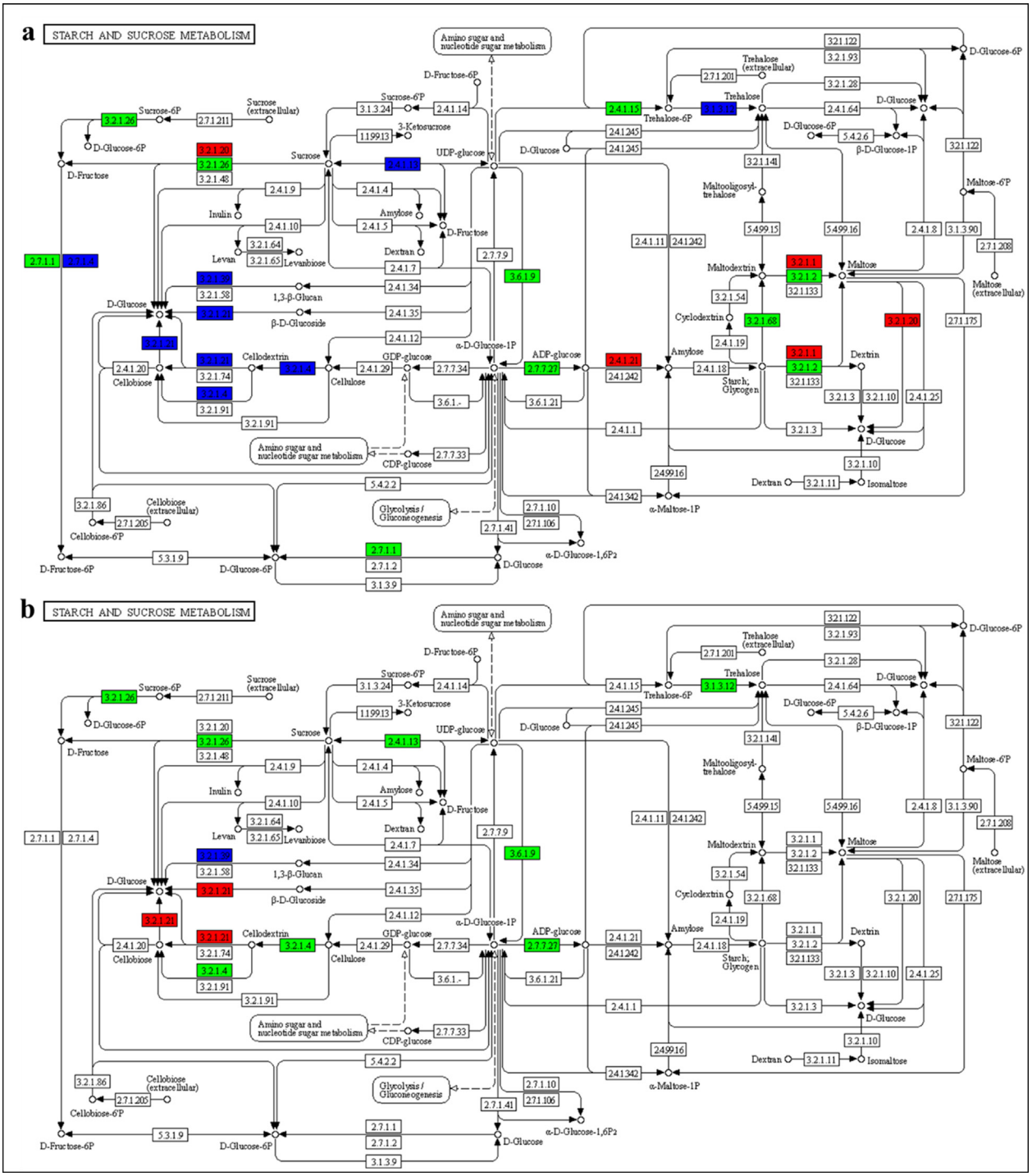

Fig. 5. Differential regulation of starch and sucrose metabolism pathway in (a) HC vs JB and (b) HC vs CB. The enzymes marked in the red, green, and blue boxes are related to the up-regulated, downregulated, and both up/downregulated genes, respectively. EC numbers correspond to the description of the genes given in Table S2 and Table S3.

and (+)-gallocatechin (i.e., leucoanthocyanidin reductase; *Cs7g12820*) was increased in JB as compared to HC. The change in the expression in these genes, and the reduced expression of other genes that are involved in the degradation of naringenin chalcone into pinobaksin 3-acetate, 5-deoxyleucopelargonidin, 5-deoxyleucocyanidin, pelagonidin, kampferol, quercetin, neohesperidin, cyanidin, and dephinidin indicate that flavonoid biosynthesis in JB was lower. This is consistent with the measured content of naringin in JB as compared to HC (Table 3; Table 4; Fig. S3a). These results are also consistent with the observation that neohesperidin content was higher in JB as compared to HC (Table 3).

The sour flavor in citrus is mainly due to citric acid and malic acid, where the former is dominant in pulp [31]. Only five DEGs were enriched in the citrate cycle between HC and JB; four were downregulated (*Cs1g03610*, *Cs1g01400*, *Cs7g21180*, and *Cs7g13790*), and one was upregulated (*Cs1g20920*) in JB. These genes are involved in the biosynthesis (and interconversion) of acetyl-coA, oxaloacetate, fumarate, succinate, and succinyl-coA. These compounds directly impact the biosynthesis of citrate and

Table 4
List of DEGs enriched in flavonoid biosynthesis pathway.

Gene ID	HC	CJ	CB	Log 2 FC (HC/CJ)	Log2 FC (HC/CB)	Gene annotation
Flavonoid biosynthesis						
Cs1g03960	57.18667	0.78	8.75	−6.223	−2.739	flavonol synthase
Cs1g12660	10.57	X	25.22	X	1.223	caffeoyl-CoA O-methyltransferase; EC:2.1.1.104
Cs1g22450	340.19	7.37	119.27	−5.56	−1.544	
Cs4g13430	9.28	24.7	X	1.379	X	
Cs6g04150	41.47	1.46	6.096	−4.857	−2.803	
Cs8g05410	42.31	13.47	X	−1.684	X	
Cs3g19360	0.72	0.11	1.99	−2.795	1.442	chalcone synthase; EC:2.3.1.74
Cs3g20330	1.34	0	X	−8.71	X	
Cs3g20680	0.26	0	X	−6.25	X	
Cs9g11190	6.37	0.58	2.67	−3.478	−1.282	
orange1.1t05430	0.27	0	0.02	−5.611	−3.89	
Cs5g11730	8.73	2.48	X	−1.845	X	flavonoid 3′-monooxygenase; EC:1.14.13.21
Cs1g19280	156.83	36.12	X	−2.151	X	flavonol synthase; EC:1.14.11.23
Cs2g04110	20.63	X	7.70	X	−1.451	
Cs3g19280	0.49	0.037	X	−3.784	X	
Cs7g12100	12.08	1.92	3.47	−2.681	−1.828	
Cs7g23280	0.21	0	X	−5.722	X	
Cs9g04630	113.74	X	48.04	X	−1.276	
Cs5g09970	2.75	0.07	X	−5.329	X	leucoanthocyanidin dioxygenase; EC:1.14.11.19
Cs6g08500	0.29	X	1.5	X	2.325	
Cs7g31010	73.03	32.11	X	−1.219	X	
Cs7g12820	0.093	0.96	X	3.291	X	leucoanthocyanidin reductase; EC:1.17.1.3
Cs1g25280	105.78	6.54	X	−4.046	X	naringenin 3-dioxygenase; EC:1.14.11.9
Cs1g19350	X	X	1.60	X	−1.182	phlorizin synthase; EC:2.4.1.357
Cs9g18780	0.23	3.82	X	4.033	X	
Cs9g18820	0.38	5.42	0.13	3.784	−1.587	
Cs9g18830	3.51	10.05	X	1.484	X	
Cs1g11780	3.48	0.34	X	−3.388	X	shikimate O-hydroxycinnamoyltransferase; EC:2.3.1.133
Cs2g30570	8.69	23.21	X	1.385	X	
Cs3g03970	12.83	1.11	X	−3.561	X	
Cs3g10440	1.79	5.78	X	1.656	X	
Cs4g02360	0.09	0.99	X	3.451	X	
Cs4g02380	0.21	2.31	X	3.453	X	
Cs4g08510	0.45	1.82	X	1.985	X	
Cs5g25860	0.06	0.34	X	2.408	X	
Cs6g12870	50.45	4.30	X	−3.588	X	
Cs6g12880	424.52	37.21	X	−3.546	X	
Cs6g17140	4.92	31.28	11.95	2.64	1.251	
Cs6g17150	0.11	0	X	−5.158	X	
Cs7g10090	3.22	8.10	X	1.297	X	
Cs7g10100	1.48	5.95	0.237	1.971	−2.679	
Cs7g10110	1.05	0.05	0.437	−4.418	−1.297	
Cs7g29080	30.17	0	0.63	−13.11	−5.612	
Cs9g08970	0.26	0	X	−6.188	X	
Cs9g11750	1.3	3.68	0.57	1.471	−1.204	
orange1.1t01192	2.07	0.19	X	−3.524	X	
orange1.1t01194	0.18	0	X	−5.53	X	
orange1.1t02793	30.91	5.59	X	−2.496	X	
orange1.1t02977	1.68	0.09	0.71	−4.208	−1.258	
orange1.1t02980	0.42	0.02	X	−4.198	X	
orange1.1t04852	0.16	0.02	0.0067	−3.224	−4.722	
Cs4g04530	4.11	0.31	0.77	−3.766	−2.443	trans-cinnamate 4-monooxygenase; EC:1.14.13.11
Citric acid and Malic acid biosynthesis						
Cs7g21180	2.49	0.63	−2.004	X	X	pyruvate dehydrogenase; EC:2.3.1.12
Cs1g20920	87.67	214.31	1.26	40.39	−1.15	phosphoenolpyruvate carboxykinase (ATP); EC:4.1.1.49
Cs1g03610	31.76	0.99	−5.021	X	X	malate dehydrogenase; [EC:1.1.1.37]
Cs1g01400	30.2	0.03	−10.89	X	X	succinate dehydrogenase; [EC:1.3.5.1]
Cs7g13790	51.21	22.97	−1.191	X	X	succinyl-CoA synthetase; [EC:6.2.1.4 6.2.1.5]

X denotes that the gene is not differentially expressed.

malate. Considering these changes, it can be understood that the citric acid and malic acid biosynthesis in JB was different than that of HC. The organic acid content estimation results are relatable as we observed higher citric acid and lower malic acid contents in JB as compared to HC (Table 2). This could affect the natural normal flavor of HC since limited quantities of citric acid and malic acid are required for leaving an acidic feel while eating citrus fruits (Table 4). A higher citric acid in JB proposes a more acidic feel than that of HC.

3.2.3.2. HC vs CB. Contrasting to HC vs JB, a relatively lower number of genes (21 as compared to 45) were differentially expressed between HC and CB. In the case of CB, we observed the downregulation of trans-cinnamate 4-monooxygenase (*Cs4g04530*) while the chalcone synthases were variedly expressed i.e., two were downregulated and one was upregulated. Interestingly, we observed that the leucoanthocyanidin reductase gene that was differentially expressed between HC and JB was not expressed in CB. Another enzyme (leucoanthocyanidin dioxygenases (*Cs5g09970* and

Cs6g08500)) that control the final steps of the biosynthesis of pelargonidin, quercetin, and cyanidin was upregulated in CB (Table 4; Fig. S3b).

Only one gene (phosphoenolpyruvate carboxykinase (ATP)) was upregulated in CB as compared to HC. The increased expression of this gene indicates that in CB, the oxaloacetate conversion to phosphoenolpyruvate is reduced (Table 4).

3.2.4. Differential regulation of genes related to mastication

3.2.4.1. HC vs JB. Mastication quality is based on mechanical properties i.e., the proportion of cell-wall-related polymers in the pulp [32]. These polymers are cellulose, hemicellulose, and pectin, and their relative proportion defines the texture and quality of the pulp in citrus fruits [33]. Our transcriptome results showed that 259 and 99 genes were differentially regulated in HC vs JB and HC vs CB, respectively. Of the pectin-related genes, we found that two probable galacturonosyltransferases (*Cs5g31870* and *Cs1g23610*), 14 pectinesterases, and nine polygalacturonases were differentially expressed between HC and JB [34]. The probable galacturonosyltransferase-like 1 s were upregulated in JB as compared to HC, whereas nine of 14 pectinesterases were downregulated in JB. Similarly, the polygalacturonases showed a variable expression pattern in JB. We also observed the upregulation of a galactan β-1,4-galactosyltransferase (*Cs2g11950*) in JB as compared to HC (Table S4).

Cellulose synthesis is governed by plasma membrane-bound cellulose synthases (CESAs) [35]. We found seven genes that were annotated as CESAs (and CESA likes; CSLs) of which four were upregulated and three were downregulated in JB as compared to HC. A CESA4, two CSL-B4s, and a CSL-E1 were upregulated in JB, while two CSL-E6s and one CSL-E1 were downregulated in JB as compared to HC. These expression changes are consistent with the observation that JB had higher cellulose content than in HC. Other enzymes that play role in cellulose synthesis such as endoglucanases were also variedly expressed in JB (Table S4).

One-third of the cell wall biomass consists of hemicelluloses. We found multiple genes annotated as xylan 1,4-β-xylosidases (three up- and one downregulated in JB), xylogalacturonan β-1,3-xylosyltransferase (upregulated in JB), xyloglucan O-acetyltransferases (four up- and four downregulated in JB), and xyloglucan:xyloglucosyl transferases (four down- and 10 upregulated in JB) in the differentially regulated genes between HC and JB (Table S4).

Only two of nine cinnamyl-alcohol dehydrogenases were upregulated in JB while the remaining seven were downregulated. Interestingly, we found seven chitinases, all of which were downregulated in JB as compared to HC (Table S4).

3.2.4.2. HC vs CB. We found 99 DEGs in CB vs HC pulp. Only 20 genes were upregulated. Notably, β-galactosidase (*Cs8g08270*), β-mannan synthase (*Cs6g15560*), glucan endo-1,3-β-glucosidase (*Cs4g08530* and *Cs8g20690*), pectinesterase (*Cs4g06630* and *Cs4g06890*), polygalacturonase (*Cs2g11570*), xyloglucan O-acetyltransferase (*Cs4g04380*), and xyloglucan:xyloglucosyl transferase (*Cs1g21130*) were upregulated in CB. However, other transcripts of the same annotation were also downregulated in CB. Regardless, we also found that two CESAs (*Cs9g08750* and *Cs4g08470*) were downregulated in CB. However, this observation is not consistent with the observed higher cellulose content in CB as compared to HC (Fig. 2c; Table S4). Since there are multiple CESAs in plants, therefore, the expression of the two observed CESAs cannot be directly linked with the observed cellulose content [36].

3.2.5. Differential regulation of genes related to pulp color

The primary pigments that impart a range of yellow to red colors in citrus pulp and peel are carotenoids, while anthocyanins give blood red color in specific orange types [13]. As there is a red color variation in JB and a yellow color variation in CB as compared to HC (Fig. 1), therefore, we explored carotenoid and anthocyanin biosynthesis-related DEGs. Thirty-one and eight genes were differentially regulated in treatment comparison HC vs JB and HC vs CB, respectively. The downregulation of 15-cis-phytoene synthase (PSY), one xanthoxin dehydrogenase (ZDS), nine zeta-carotene desaturases (ZISOs), and zeaxanthin epoxidases (ZEPs) in JB indicates that the synthesis of phytoene followed by its conversion into lycopene, and ultimately to xanthoxin was lower than HC. However, we also found increased expression of 9-cis-epoxycarotenoid deoxygenase (NCED), TWO ZDSs, and four ZISOs in JB. In CB, a small number of genes related to carotenoid biosynthesis were differentially expressed; one PSY, three NCEDs, one abscisic-aldehyde oxidase (AAO), one ZDS, and two ZEPs (Fig. 6).

Only one DEG (anthocyanidin 3-O-glucosyltransferase; *Cs4g02990*) was enriched in the anthocyanin biosynthesis pathway. This gene was downregulated both in JB (-6.027) and CB (-2.174) as compared to HC.

3.3. Metabolic profiles of HC, JB, and CB

To identify the differentially accumulated metabolites in three fruits' pulps, we applied a series of OPLS-DA to maximize the discrimination between the samples and focus on the variation in compounds significantly contributing to the resulting classifications. The OPLS-DA showed that significant biochemical variation existed between the tested pulp types (Fig. S5). This was also evident from the grouping of the treatment replicates together, and the separate grouping of replicates from different treatments in the PCA plot (Fig. S5).

A total of 283 and 94 metabolites were differentially accumulated in treatment comparisons HC vs JB and HC vs CB, respectively; 69 DAMs were common in both treatment comparisons (Fig. 6; Table S5). The DAMs in HC vs JB were enriched in multiple pathways as shown in Fig. 7. The accumulated metabolites were classified as flavonoids, lipids, lignans and coumarins, alkaloids, organic acids, amino acids and derivatives, nucleotides and derivatives, and tannins and quinones (Fig. 8).

3.3.1. Differentially accumulated metabolites between HC and JB

Four metabolites i.e., scopoletin (7-Hydroxy-5-methoxycoumarin), gardenin B, diosmetin (5,7,3′-Trihydroxy-4′-methoxyflavone), and D-panthenol were accumulated exclusively in JB as compared to HC. Contrastingly, 52 metabolites were exclusively accumulated in HC as compared to JB (Table S5). These differential changes suggest a reduced metabolic activity in JB as compared to HC. Of the 283 DAMs, 194 had reduced accumulation in JB as compared to HC. Particularly, we found that saccharides and alcohols (7 of 10) had lower content in JB suggesting reduced sugar contents in it. Two compounds i.e., fumaric acid and succinic acid (enriched in the citric acid cycle) had lower contents in JB as compared to HC. Similar accumulation trend was observed for other organic acids. Nonetheless, the concentration of only four organic acids i.e., 1-Aminocyclopropane-1-carboxylic acid, citraconic acid, 2-Hydroxy-3-phenylpropanoic acid, and quinic acid were higher in JB as compared to HC. One particular observation was the reduced accumulation of most of the phenolic acids (Table S5). Regarding the bitterness, the metabolome comparison also revealed that naringenin chalcone and naringenin-7-O-Rutino side-4′-O-glucoside had lower content in JB as compared to HC.

Compounds related to cell wall such as lignans and coumarins were also differentially accumulated between HC and JB. Two

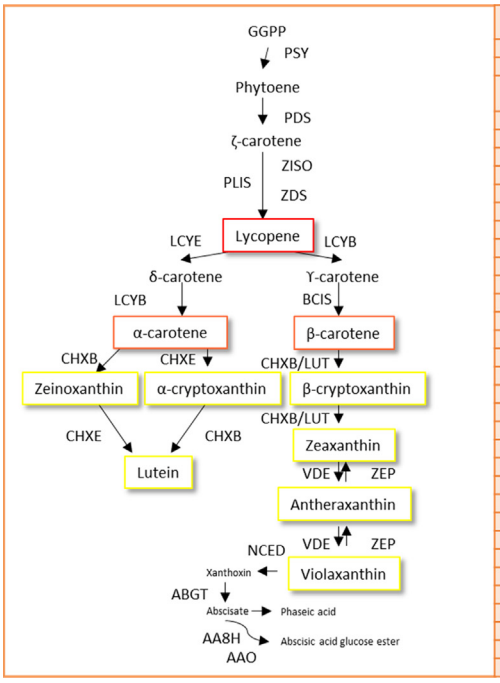

ID	HC FPKM	JB FPKM	CB FPKM	Log2 FC HC/JB	Log2 FC HC/CB	KEGG
Cs3g23530	0.57	3.196667	X	2.466	X	(+)-abscisic acid 8'-hydroxylase; AA8H
Cs8g18780	2.69	0.21	X	-3.71	X	(+)-abscisic acid 8'-hydroxylase; AA8H
orange1.1t02108	11.17666667	0.313333	1.646666667	-5.202	-2.795	15-cis-phytoene/all-trans-phytoene synthase ; PSY
Cs7g14820	1.366666667	X	4.003333333	X	1.514	9-cis-epoxycarotenoid dioxygenase; NCED
Cs8g14150	0.203333333	X	1.123333333	X	2.428	9-cis-epoxycarotenoid dioxygenase; NCED
Cs6g19500	0.1	0.873333	X	3.092	X	9-cis-epoxycarotenoid dioxygenase ; NCED
Cs9g11260	7.263333333	0	7.263333333	-11.478	-1.271	9-cis-epoxycarotenoid dioxygenase ; NCED
Cs8g05320	0.743333333	0.343333	X	-1.153	X	abscisate beta-glucosyltransferase; ABGT
Cs8g13780	0.253333333	X	0.623333333	X	1.26	abscisic-aldehyde oxidase; AAO
Cs8g13770	3.54	1.636667	X	-1.146	X	abscisic-aldehyde oxidase ; AAO
Cs1g04080	2.843333333	9.69	X	1.739	X	violaxanthin de-epoxidase ; ZDS
Cs6g09480	4.686666667	0.186667	4.686666667	-4.686	-3.199	xanthoxin dehydrogenase; ZDS
Cs7g04930	0.853333333	1.923333	X	1.141	X	xanthoxin dehydrogenase ; ZDS
Cs1g04870	164.75	5.646667	164.75	-4.899	-1.073	zeaxanthin epoxidase; ZEP
Cs4g20530	1.03	0.156667	X	-2.777	X	zeaxanthin epoxidase ; ZEP
Cs4g20550	1.866666667	0.65	X	-1.554	X	zeaxanthin epoxidase ; ZEP
Cs4g20560	1.316666667	0.466667	X	-1.524	X	zeaxanthin epoxidase ; ZEP
Cs4g20590	2.366666667	0.223333	X	-3.45	X	zeaxanthin epoxidase ; ZEP
orange1.1t04051	0.193333333	0.003333	X	-5.315	X	zeaxanthin epoxidase ; ZEP
orange1.1t04849	0.22	0	X	-5.607	X	zeaxanthin epoxidase ; ZEP
orange1.1t05125	0.786666667	0.016667	0.786666667	-5.78	-3.516	zeaxanthin epoxidase ; ZEP
Cs1g18980	0.106666667	0.39	X	1.852	X	zeta-carotene desaturase; ZISO
Cs3g11000	2.23	5.976667	X	1.385	X	zeta-carotene desaturase; ZISO
Cs3g11090	6.023333333	1.893333	X	-1.706	X	zeta-carotene desaturase ; ZISO
Cs3g11120	0.423333333	0.053333	X	-3.013	X	zeta-carotene desaturase ; ZISO
Cs3g12720	0.94	0.166667	X	-2.508	X	zeta-carotene desaturase ; ZISO
Cs3g12740	0.603333333	0.04	X	-4.042	X	zeta-carotene desaturase ; ZISO
Cs3g12760	1.746666667	0.67	X	-1.424	X	zeta-carotene desaturase ; ZISO
Cs3g12810	1.303333333	0.32	X	-2.057	X	zeta-carotene desaturase ; ZISO
Cs6g02150	2.95	1.083333	X	-1.473	X	zeta-carotene desaturase ; ZISO
Cs6g06810	3.15	0.873333	X	-1.878	X	zeta-carotene desaturase ; ZISO
orange1.1t04537	2.223333333	0.696667	X	-1.711	X	zeta-carotene desaturase ; ZISO
orange1.1t05193	0.063333333	0.566667	X	3.095	X	zeta-carotene desaturase ; ZISO
orange1.1t05295	0	0.15	X	4.859	X	zeta-carotene desaturase ; ZISO

Fig. 6. Carotenoid biosynthesis pathway and differentially expressed DEGs in treatment comparisons HC vs JB and HC vs CB. The X represents that the genes are not differentially expressed.

lignans (Pinoresinol-4-O-glucoside and syringaresinol-4′-O-(6′′-acetyl) glucoside), and five coumarins and lignans (umbelliferone, 6,7-Dihydroxy-4-methylcoumarin, Scopoletin (7-Hydroxy-5-methoxycoumarin), scopoletin-7-O-glucuronide, and N-Sinapoylhydroxycoumarin) were increasingly accumulated in JB as compared to HC (Table S5).

The metabolome comparison showed that all the detected anthocyanins had reduced contents in JB.

3.3.2. Differentially accumulated metabolites between HC and CB

The metabolome comparison between HC and CB revealed that 44 and 50 compounds were accumulated in higher quantities in CB and HC, respectively. Moreover, 10 metabolites were exclusively accumulated in HC; dopamine, citrusin I, umbelliferone, 6-C-MethylKaempferol-3-glucoside, kaempferol-3-O-(2′′-O-acetyl) glucuronide, sinapyl alcohol, neochlorogenic acid (5-O-caffeoylquinic acid), chlorogenic acid methyl ester, 5-O-geruloylquinic acid, and bis(p-coumaroyl) tartaric acid. Contrastingly, only three metabolites were exclusive to CB i.e., Scopoletin (7-Hydroxy-5-methoxycoumarin), gardenin B, and D-panthenol. The exclusive metabolites with CB are common with JB, indicating that these metabolites might be playing role in changes in pulp color, mastication, and taste. Only three saccharides and alcohols i.e., gluconic acid, D-panthenol, and sedoheptulose were differentially accumulated in HC vs CB. These three metabolites were detected in higher quantities in CB as compared to HC. Alkaloids, amino acids, and derivatives had mixed regulation i.e., some were accumulated higher in HC while others had higher concentrations in CB. Though most phenolic acids had lower content in CB, we found that disinapoyl glucoside, isochlorogenic acid, methyl sinapate, and 1-O-vanilloyl-D-glucose had higher contents in CB. Similar to phenolic acids, flavonoids were also highly accumulated in HC except for dihydroflavones, which showed higher accumulation in CB. Similarly, almost all flavanols accumulated in higher quantities in CB except isorhamnetin-3-O-Glucoside and kaempferol-3-O-(2′′-O-acetyl) glucuronide. Regarding pigments, three of four anthocyanins had lower contents while petunidin-3-O-rutinoside content was higher in CB than HC (Table S5). The anthocyanin contents decreased and increased accumulation of petunidin-3-O-rutinoside in CB might be possible reasons for yellow coloration in its pulp as compared to HC.

3.4. Combined transcriptome and metabolome analysis

The joint mapping of DEGs and DAMs on the KEGG pathways showed their significant enrichment on multiple pathways in both treatment comparisons i.e., HC vs JB and HC vs CB (Table S3). Interestingly, the pathways in which DEGs and DAMs were enriched combinedly were mostly the same as of separate KEGG pathway enrichment analysis. The DAMs and DEGs having PCC $\leq$ 8 were chosen to see variation between the both (Fig. 9).

4. Discussion

4.1. Possible roles of sugar, citric acid, and flavonoid biosynthesis pathways in the taste variation between HC, JB, and CB

The nutritional status of oranges makes them an attractive fruit for human consumption. They are considered a good source of vitamins, minerals, and dietary fibers as well as pharmacologically important phytochemicals such as flavonoids, carotenoids, and organic acids [37]. The citrus fruit pulp is the source of most of these nutrients and is directly consumed. Although the oranges are liked by different individuals differently, the actual pulp taste is developed due to an appropriate balance between sweetness and sourness [38]. The sweetness in citrus pulp is mainly due to the soluble sugars i.e., sucrose, fructose, and glucose. Sucrose synthesized in leaves arrives in the pulp (reservoir) from leaves, where it is converted into fructose and glucose or fructose and UDP glucose [39]. In both JB and CB pulps, the differential regulation of key sugar biosynthetic genes is consistent with the reduced soluble sugar content in these two fruit variants. Particularly, changes in the expression of fructose and mannose metabolism indicate that fructose is being degraded. At the same time, the steps that

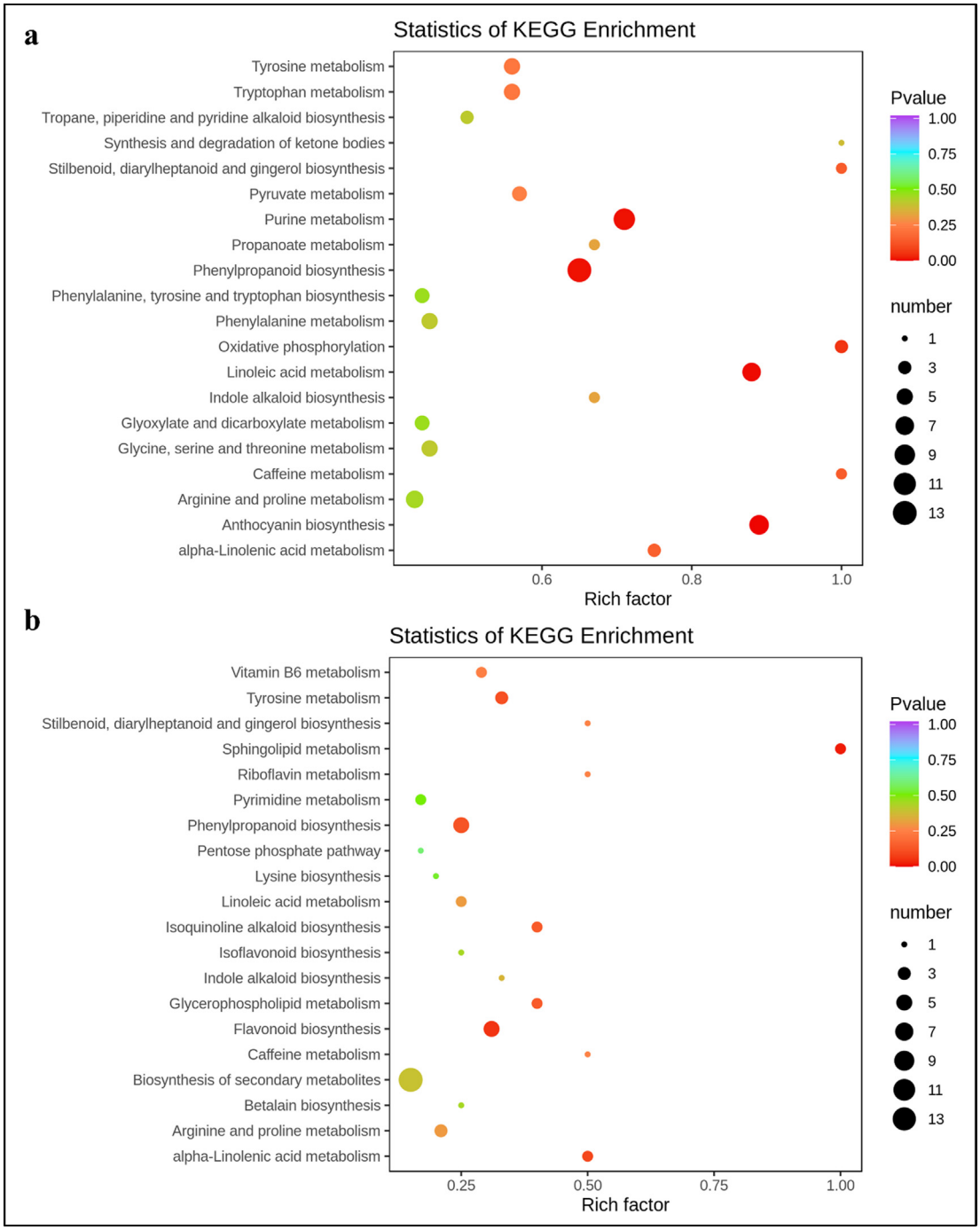

Fig. 7. KEGG pathways in which the metabolites were enriched in HC vs JB and HC vs CB.

connect this pathway with organic acid metabolism i.e., the degradation of β-D-fructose 6P into glyceraldehyde-3P and/or the interconversion of D-fructose 1P and glycerone-P were downregulated, which resulted in reduced supplies to the organic acid biosynthesis pathway [38]. This follows the modified accumulation of most of the organic acids in JB (Table 2; Table S5). This could cause a change in the flavor since the nature and concentration of the organic acids largely affect the taste and organoleptic characteristics [40]. Thus, an overall reduced fructose level in JB and CB should be causing a reduced sweet taste as compared to HC. We say this because in case of HC, the conversion of arriving sucrose into D-fructose and D-glucose (as evident from regulation of the key genes) was observed, while in JB and CB, multiple enzymes in sugar-related pathways had differential expression (Fig. 5). This is further supported by the fact that the SUSs were downregulated in both JB and CB, which resulted in a reduced sucrose synthesis (Table S2). These observations are consistent with the metabolite profiles where saccharides and alcohols had lower content in JB (Table S5). This is further supported by the observed changes in soluble sugar contents (Fig. 2). UDP sugars are also produced from GlcNAc, and the downregulation of hexokinases, glucosamine-fructose-6-phosphate aminotransferase, cytochrome-b5 reductase, reversibly glycosylated polypeptide/UDP-arabinopyranose mutase, α-N-arabinofuranosidase, and UDPglucose 6-dehydrogenas

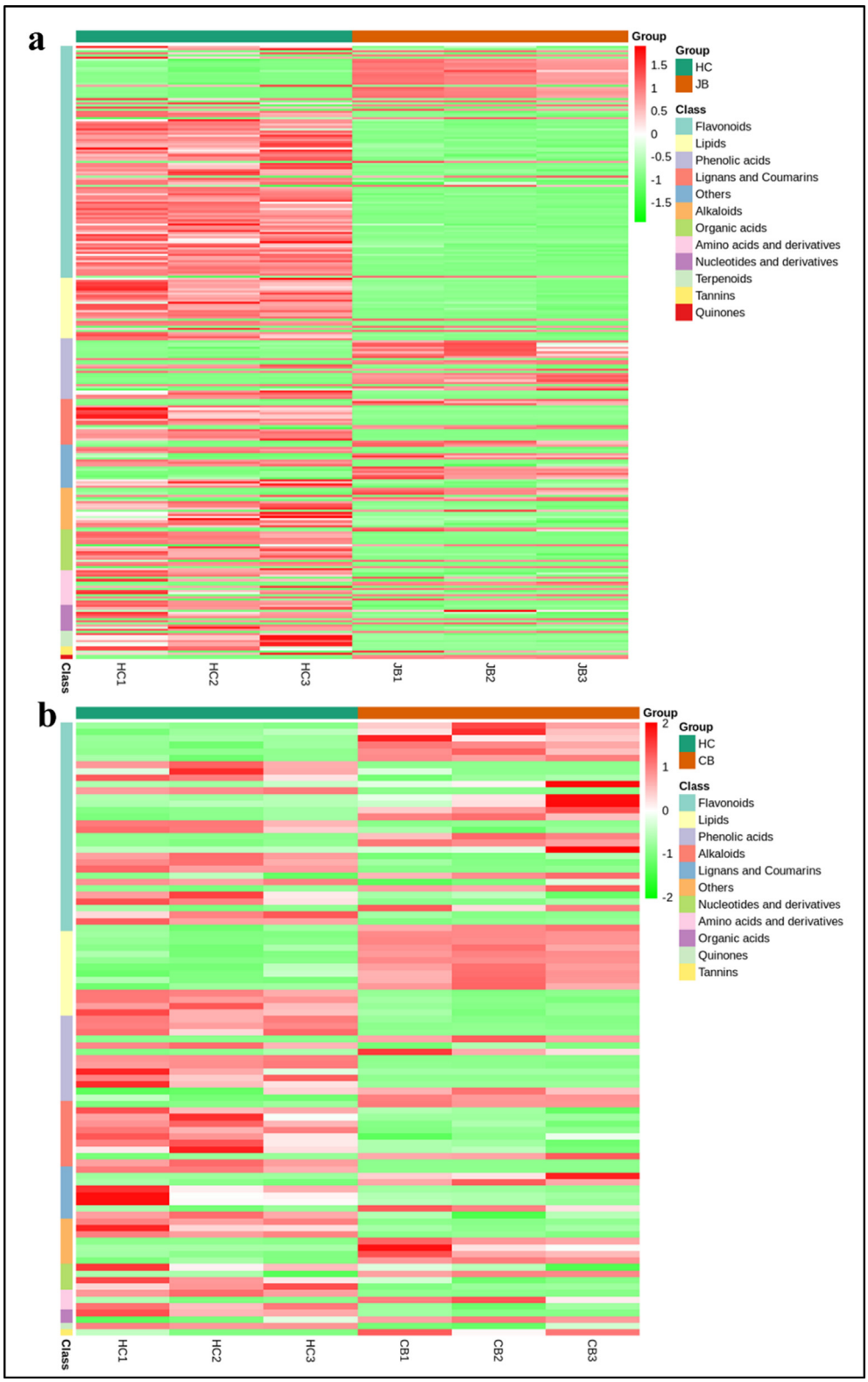

Fig. 8. Heatmap of the differentially accumulated metabolites in (a) HC vs JB and (b) HC vs CB.

indicated lower UDP sugars [41]. Overall, we can conclude that in JB and CB, the sugar content is reduced as compared to HC. Since taste is not only the sugar content but also includes bitterness and sourness-related biochemical changes, therefore, considering citrate and citric acid is an important way to look for favorable taste. In this regard, the relatively higher expression of phosphoenolpyruvate carboxykinase (ATP) in JB and lower expression in CB indicates that citrate released during ripening is increased in JB and decreased in CB. However, further studies on the specific changes in response to the differential expression of this enzyme could shed light on the downstream pathways and products. Since, we differential regulation of most of the genes that lead toward the

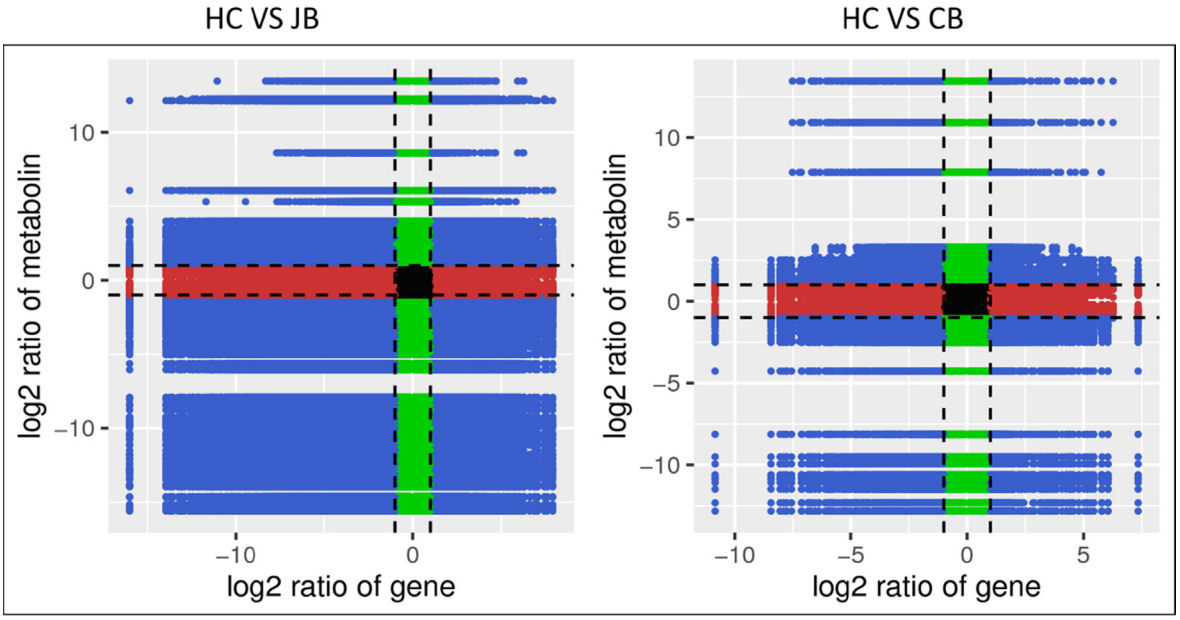

Fig. 9. Nine-quadrant diagram of the Pearson correlation coefficient between DEGs and DAMs in treatment comparisons HC vs JB and HC vs CB. Black dots = unchanged genes/metabolites, green dots = DAMs with unchanged genes, red dots = DEGs with unchanged metabolites, blue dots = DEGs and DAMs.

biosynthesis of α-D-glucose 1P (a key product connecting glycolysis/gluconeogenesis and sucrose and starch biosynthesis pathways [42]), together with the expression changes in the sugars biosynthesis/degradation-related genes, could be an important reason for taste variation in JB and CB (Fig. 5; Fig. S2; Table S5). Finally, the flavonoids (particularly naringin) and flavanone-neohesperidosides cause a bitter taste in citrus fruits [42]. The reduced expression of trans-cinnamate 4-monooxygenase and chalcone synthases in both JB and CB indicate that HC and its variants have possibly lower naringin levels (probably that is why normal HC fruit is favored by consumers). We say this because in both treatment comparisons, we did not find differentially expressed naringenin 7-O-glucosyltransferase and flavanone 7-O-glucoside 2′′-O-β-L-rhamnosyltransferase, which synthesize naringin from naringenin in two successive steps [43]. Instead, the conversion of naringenin (and its biosynthesis) into other products leading to anthocyanin biosynthesis was observed (Table 3; Fig. S3). These observations are consistent with the metabolome results where we found lower contents of naringenin chalcone and naringenin-7-O-Rutinoside-4′-O-glucoside in JB and higher naringenin (5,7,4′-Trihydroxyflavanone) contents in CB (Table S5). Taken together, the reduced/altered expression of genes enriched in sugar-related pathways, citrate cycle, and flavonoid biosynthesis pathway is the main variation leading to taste the difference in HC, JB, and CB.

4.2. Differential regulation of mastication in HC, JB, and CB

Mastication and fruit texture are important quality traits that are associated with the mechanical properties of citrus fruits [44]. The cell wall polymers i.e., cellulose and hemicellulose are the key components of the mechanical properties of citrus fruits. However, studies have also reported that pectin (protopectin) and lignin content are major determinants of the fruit mastication trait in citrus e.g., in *Citrus reticulata* [45]. The final texture of the fruit pulp is developed when protopectin is completely or partially solubilized or depolymerized. In this regard, the expression of polygalacturonase can be an indication of catabolism of pectin [46]. Thus, the downregulation of polygalacturonases in JB and CB indicates the reduced fine texture in both fruit pulps. Additionally, pectinesterases are also key players in mastication. A study revealed that fruits with superior mastication traits have higher expression levels of both polygalacturonases and pectinesterases [45]. Our results are consistent with this report since we found that polygalacturonases and pectinesterases were downregulated in JB and CB suggesting that these fruit pulps have reduced mastication as compared to HC. This statement is further supported by the results where we observed a higher expression of CESA4 in JB (Table S4), which is possibly contributing to the increased cellulose content [35]. This has been previously confirmed by multiple studies which reported that a higher cellulose content is responsible for hard mastication and coarse taste in the mouth [47]. Plant MYB transcription factors have also been implicated in cell wall modification and affecting the mastication trait in *C. sinensis* [48]. The upregulation of two MYBs in each JB pulp type and CB pulp type is indicative of the regulation of lignin, xylan, and cellulose biosynthesis [49]. The observed accumulation of metabolites that were annotated as coumarins and lignans e.g., umbelliferone, 6,7-Dihydroxy-4-methylcoumarin, and scopoletin (7-Hydroxy-5-methoxycoumarin) is indicative of modification in the cell wall in JB and CB. These metabolites have been characterized for their roles in cell wall modification [50]. Taken together, our transcriptome and metabolome analysis indicate that mastication in JB and CB is inferior to HC due to the changes in the expression of genes and metabolites related to cell wall polymers.

4.3. Anthocyanin and carotenoid biosynthesis variation in HC, JB, and CB

Citrus pulp color is developed due to the accumulation and differential composition of anthocyanin and carotenoids [51], since we observed that the expression of the ZYS, ZDS and ZISO was higher in HC, which could be indicative of higher production of pigments in HC giving it a yellowish and reddish pulp color (Fig. 6). This statement is further supported by the result that the ZEPs had higher expression in HC. ZEP is responsible for the interconversion of zeaxanthin, violaxanthin, and antheraxanthin [52]. These three pigments give characteristic yellow color to the plant tissue; therefore, the higher expression of ZYS, ZDS, ZISO, and ZEPs in HC is probably the cause of the yellowish and reddish color in the pulp. The upregulation of some genes like 9-cis-epoxycarotenoid deoxy-

genase (NCED), TWO ZDSs, and four ZISOs in JB indicate that lycopene biosynthesis is higher, which is giving a slightly orange color to JB pulp [53]. The different number of genes having variable expression could be due to the ongoing expression changes in different sections of the pulp or its different sides since it can be seen that some parts of the HC fruit are still yellowish while a larger portion is orange in color (Fig. 1). The pulp of CB fruit was standard yellow pulp color. Since we did not detect a large number of DEGs in CB that were related to this pathway, therefore, it could be stated that the xanthin, lycopene, or carotene pigment biosynthesis is affected. We say this because we noted the relatively increased expression of genes such as NCED, ZDS and AAO. These expression changes also hint toward the accumulation of yellow pigments in CB. The only DEG in HC vs CB i.e., anthocyanidin 3-O-glucosyltransferase converts the three anthocyanins (cyanidin, pelargonidin, and delphinidin) into their respective 3-O-glucosides (Table S4). Both cyanidin 3-O-glucoside and pelargonidin 3-O-glucosides have reddish colors [54,55]. Hence, higher expression of this gene in HC can be related to the slightly orange color in its pulp. We say this because we observed another gene that was enriched in the flavonoid biosynthesis pathway i.e., leucoanthocyanidin dioxygenase, which biosynthesizes the anthocyanin and protoanthocyanidins by catalyzing the oxidation of leucoanthocyanidins into anthocyanidins [56]. Therefore, its upregulation in JB indicates increased production of leucopelargonidin, leucocyanidin, leucodelphinidin, pelargonidin, cyanidin, and delphinidin in pulp, thus giving the orange color. Considering both the transcriptome results and metabolites detected in JB and CB, we can conclude that the color of HC is due to the carotenoid biosynthesis pathway regulation and the variation in color of JB and CB is due to the differential regulation of both carotenoid and anthocyanin biosynthesis.

5. Conclusions

The two HC variants i.e., JB and CB have different flavonoid, organic acid, soluble protein, soluble sugar, and cellulose content. The transcriptome and metabolome analyses of HC and its two variants (JB and CB) showed that sugar and organic acid biosynthesis pathways were differentially regulated between the three fruit pulps. These changes are predicted to affect the taste of JB and CB. Particularly, starch and sucrose biosynthesis, citrate cycle, fructose and mannose metabolism, galactose metabolism, glycolysis/gluconeogenesis are key pathways that lead to the changes in the flavor of *C. sinensis* (HC, JB, and CB). The mastication characteristics of HC were superior to JB and CB as evident from the reduced expression of polygalacturonases and pectinesterases, increased expression of CESAs and MYB transcription factors, and differential accumulation of coumarins and lignans in JB and CB as compared to HC. Finally, the color variation in JB and CB compared to HC is due to the regulation of anthocyanin and carotenoid biosynthesis pathways. Our results lay down the foundations for studying and expanding the knowledge on the differences in the citrus chimeras and their variants.

Authors contributions

- Study conception and design: Z Yang, X Cao, F Feng, C Ye
- Data collection: Z Yang, X Cao, X Zheng
- Analysis and interpretation of results: Z Yang, X Cao, X Zheng, T Wang, J Wang
- Draft manuscript preparation: Z Yang, X Cao
- Revision of the results and approved the final version of the manuscript: Z Yang, X Cao, X Zheng, T Wang, J Wang, F Feng, C Ye

Financial support

This work was funded by the Provincial Science and Technology Innovation Strategy Special Fund Competitive Allocation Project (2018A03016). The study was also supported by the project funded by Innovation and Strong School Project (2018KTSCX085) and China's National 13th Five-Year Key R&D Program (2019YFD1002205). The funders had no role in study design, data collection and analysis, decision to publish, or preparation of the manuscript.

Conflicts of Interest

The authors declare no conflict of interest.

Supplementary material

https://doi.org/10.1016/j.ejbt.2022.09.001.

References

[1] Li J, Chen J. Citrus fruit-cracking: Causes and occurrence. Hortic Plant J 2017;3(6):255–60. https://doi.org/10.1016/j.hpj.2017.08.002.
[2] Xu Q, Chen L-L, Ruan X, et al. The draft genome of sweet orange (*Citrus sinensis*). Nat Genet 2013;45(1):59–66. https://doi.org/10.1038/ng.2472. PMid: 23179022.
[3] Foster TM, Aranzana MJ. Attention sports fans! The far-reaching contributions of bud sport mutants to horticulture and plant biology. Hort Res 2018;5(1):44. https://doi.org/10.1038/s41438-018-0062-x. PMid: 30038785.
[4] Zhang M, Zhang Z, Wu Q, et al. Chimerism Evaluation of 'Hongrou Huyou', a Grafted Chimera between *Citrus changshan-huyou* and *Citrus unshiu*. Horticult Sci Technol 2020;38(1):107–17. https://doi.org/10.7235/HORT.20200011.
[5] Zhang M, Deng X, Qin C, et al. Characterization of a new natural periclinal navel–Satsuma chimera of Citrus: 'Zaohong'navel orange. J Am Soc Hort Sci 2007;132(3):374–80, https://doi.org/10.21273/JASHS.132.3.374.
[6] Chen J, Yuan Z, Zhang H, et al. *Cit 1, 2Rha*T and two novel *CitdGlcT*s participate in flavor-related flavonoid metabolism during citrus fruit development. J Exp Bot 2019;70(10):2759–71. https://doi.org/10.1093/jxb/erz081. PMid: 30840066.
[7] Feng S, Suh JH, Gmitter FG, et al. Differentiation between flavors of sweet orange (*Citrus sinensis*) and mandarin (*Citrus reticulata*). J Agric Food Chem 2018;66(1):203–11. https://doi.org/10.1021/acs.jafc.7b04968. PMid: 29237265.
[8] Le Lievre D, Anderson R, Boldingh H, et al. Modifying Carbohydrate Supply to Fruit during Development Changes the Composition and Flavour of *Actinidia chinensis* var. *chinensis* 'Zesy002' Kiwifruit. Plants 2021;10(7):1328. https://doi.org/10.3390/plants10071328. PMid: 34209861.
[9] Arena ME, Zuleta A, Dyner L, et al. *Berberis buxifolia* fruit growth and ripening: Evolution in carbohydrate and organic acid contents. Sci Hortic 2013;158:52–8. https://doi.org/10.1016/j.scienta.2013.04.026.
[10] Lado J, Gambetta G, Zacarias L. Key determinants of citrus fruit quality: Metabolites and main changes during maturation. Sci Hortic 2018;233:238–48. https://doi.org/10.1016/j.scienta.2018.01.055.
[11] Goldenberg L, Yaniv Y, Porat R, et al. Mandarin fruit quality: A review. J Sci Food Agri 2018;98(1):18–26. https://doi.org/10.1002/jsfa.8495. PMid: 28631804.
[12] Xiong Y, Yan P, Du K, et al. Nutritional component analyses of kiwifruit in different development stages by metabolomic and transcriptomic approaches. J Sci Food Agri 2020;100(6):2399–409. https://doi.org/10.1002/jsfa.10251. PMid: 31917468.
[13] Chen C, Lo Piero AR, Gmitter F, Chen C. Pigments in citrus. In: Chen C, editor. Pigments in fruits and vegetables. New York, NY: Springer; 2015. p. 165–87. https://doi.org/10.1007/978-1-4939-2356-4_8.
[14] Rodrigo MJ, Alquézar B, Alós E, et al. Biochemical bases and molecular regulation of pigmentation in the peel of Citrus fruit. Sci Hortic 2013;163:46–62. https://doi.org/10.1016/j.scienta.2013.08.014.
[15] Lu X, Cao X, Li F, et al. Comparative transcriptome analysis reveals a global insight into molecular processes regulating citrate accumulation in sweet orange (*Citrus sinensis*). Physiol Plantarum 2016;158(4):463–82. https://doi.org/10.1111/ppl.12484. PMid: 27507765.
[16] Tian J, Feng S, Liu Y, et al. Single-molecule long-read sequencing of *Zanthoxylum bungeanum* Maxim. transcriptome: identification of aroma-related genes. Forests 2018;9(12):765. https://doi.org/10.3390/f9120765.
[17] Liew SS, Ho WY, Yeap SK, et al. Phytochemical composition and *in vitro* antioxidant activities of *Citrus sinensis* peel extracts. PeerJ 2018;6:5331. https://doi.org/10.7717/peerj.5331. PMid: 30083463.
[18] Grintzalis K, Georgiou CD, Schneider Y-J. An accurate and sensitive Coomassie Brilliant Blue G-250-based assay for protein determination. Analyt Biochem 2015;480:28–30. https://doi.org/10.1016/j.ab.2015.03.024. PMid: 25837770.

[19] Wu L-M, Wang C, He L-G, et al. Transcriptome analysis unravels metabolic and molecular pathways related to fruit sac granulation in a late-ripening navel orange (*Citrus sinensis* Osbeck). Plants 2020;9(1):95. https://doi.org/10.3390/plants9010095. PMid: 31940826.
[20] Chen L, Wu Q, He W, et al. Combined De Novo Transcriptome and Metabolome Analysis of Common Bean Response to *Fusarium oxysporum* f. sp. *phaseoli* Infection. Int J Mol Sci 2019;20(24):6278. https://doi.org/10.3390/ijms20246278. PMid: 31842411.
[21] Kim D, Paggi JM, Park C, et al. Graph-based genome alignment and genotyping with HISAT2 and HISAT-genotype. Nature Biotechnol 2019;37(8):907–15. https://doi.org/10.1038/s41587-019-0201-4. PMid: 31375807.
[22] Gel B, Serra E. karyoploteR: an R/Bioconductor package to plot customizable genomes displaying arbitrary data. Bioinformatics 2017;33(19):3088–90. https://doi.org/10.1093/bioinformatics/btx346. PMid: 28575171.
[23] Liao Y, Smyth GK, Shi W. featureCounts: an efficient general purpose program for assigning sequence reads to genomic features. Bioinformatics 2014;30(7):923–30. https://doi.org/10.1093/bioinformatics/btt656. PMid: 24227677.
[24] Benjamini Y, Hochberg Y. Controlling the false discovery rate: a practical and powerful approach to multiple testing. J Roy Stat Soc: Ser B (Methodol) 1995;57(1):289–300. https://doi.org/10.1111/j.2517-6161.1995.tb02031.x.
[25] Love MI, Huber W, Anders S. Moderated estimation of fold change and dispersion for RNA-seq data with DESeq2. Genome Biol 2014;15(12):550. https://doi.org/10.1186/s13059-014-0550-8. PMid: 25516281.
[26] Kukurba KR, Montgomery SB. RNA sequencing and analysis. Cold Spring Harbor Protocols 2015;2015(11):951–69. https://doi.org/10.1101/pdb.top084970. PMid: 25870306.
[27] Chong J, Xia J. MetaboAnalystR: an R package for flexible and reproducible analysis of metabolomics data. Bioinformatics 2018;34(24):4313–4. https://doi.org/10.1093/bioinformatics/bty528. PMid: 29955821.
[28] Xie C, Mao X, Huang J, et al. KOBAS 2.0: a web server for annotation and identification of enriched pathways and diseases. Nucleic Acids Res 2011;39(suppl_2):W316–22. https://doi.org/10.1093/nar/gkr483. PMid: 21715386.
[29] Fukushima A. DiffCorr: an R package to analyze and visualize differential correlations in biological networks. Gene 2013;518(1):209–14. https://doi.org/10.1016/j.gene.2012.11.028. PMid: 23246976.
[30] Frydman A, Liberman R, Huhman DV, et al. The molecular and enzymatic basis of bitter/non-bitter flavor of citrus fruit: evolution of branch-forming rhamnosyltransferases under domestication. The Plant J 2013;73(1):166–78. https://doi.org/10.1111/tpj.12030. PMid: 22989156.
[31] Etienne A, Génard M, Lobit P, et al. What controls fleshy fruit acidity? A review of malate and citrate accumulation in fruit cells. J Exp Bot 2013;64(6):1451–69. https://doi.org/10.1093/jxb/ert035. PMid: 23408829.
[32] Forlani S, Masiero S, Mizzotti C. Fruit ripening: the role of hormones, cell wall modifications, and their relationship with pathogens. J Exp Bot 2019;70(11):2993–3006. https://doi.org/10.1093/jxb/erz112. PMid: 30854549.
[33] Colodel C, Vriesmann LC, Petkowicz CLO. Cell wall polysaccharides from Ponkan mandarin (*Citrus reticulata* Blanco *cv. Ponkan) peel*. Carbohyd Polym 2018;195:120–7. https://doi.org/10.1016/j.carbpol.2018.04.066. PMid: 29804959.
[34] Nawaz MA, Rehman HM, Imtiaz M, et al. Systems identification and characterization of cell wall reassembly and degradation related genes in Glycine max (L.) Merill, a bioenergy legume. Sci Rep 2017;7(1):10862. https://doi.org/10.1038/s41598-017-11495-4. PMid: 28883533.
[35] Nawaz MA, Lin X, Chan T-F, et al. Characterization of cellulose synthase A (CESA) gene family in eudicots. Biochem Genet 2019;57(2):248–72. https://doi.org/10.1007/s10528-018-9888-z. PMid:30267258.
[36] Little A, Schwerdt JG, Shirley NJ, et al. Revised phylogeny of the *Cellulose synthase* gene superfamily: Insights into cell wall evolution. Plant Physiol 2018;177(3):1124–41. https://doi.org/10.1104/pp.17.01718. PMid: 29780036.
[37] Gyawali R, Kim KS. Anticancer phytochemicals of citrus fruits—A review. J Animal Res 2014;4(1):85–95. https://doi.org/10.5958/2277-940X.2014.00079.5.
[38] Baldwin EA, Bai J, Plotto A, et al. Citrus fruit quality assessment; producer and consumer perspectives. Stewart Postharvest Rev 2014;10(2).
[39] Li L-J, Tan W-S, Li W-J, et al. Citrus taste modification potentials by genetic engineering. Int J Mol Sci 2019;20(24):6194. https://doi.org/10.3390/ijms20246194. PMid: 31817978.
[40] Carvalho DU, Da Cruz MA, Colombo, et al. Determination of organic acids and carbohydrates in 'Salustiana' orange fruit from different rootstocks. Brazilian. J Food Technol 2020;23: e2018329. https://doi.org/10.1590/1981-6723.32918.
[41] Decker D, Kleczkowski LA. UDP-sugar producing pyrophosphorylases: Distinct and essential enzymes with overlapping substrate specificities, providing *de novo* precursors for glycosylation reactions. Front Plant Sci 2019;9:1822. https://doi.org/10.3389/fpls.2018.01822 PMid: 30662444.
[42] Sharabi K, Tavares CD, Rines AM, et al. Molecular pathophysiology of hepatic glucose production. Mol Aspects Med 2015;46:21–33. https://doi.org/10.1016/j.mam.2015.09.003 PMid: 26549348.
[43] Sharma P, Kumar V, Guleria P. Naringin: Biosynthesis and pharmaceutical applications. Indian J Pharmac Sci 2019;81(6):988–99. https://doi.org/10.36468/pharmaceutical-sciences.596.
[44] Liu Y-Z, Dong T, Lei Y, et al. Isolation of a polygalacturonase gene from *Citrus sinensis* fruit and its expression relative to fruit mastication trait, fruit development, and calcium or boron treatments. Plant Mol Biol Rep 2011;29(1):51–9. https://doi.org/10.1007/s11105-010-0206-0.
[45] Lei Y, Liu YZ, Gu QQ, et al. Comparison of cell wall metabolism in the pulp of three cultivars of 'Nanfeng' tangerine differing in mastication trait. J Sci Food Agri 2012;92(3):496–502. https://doi.org/10.1002/jsfa.4554 PMid: 21732384.
[46] Molinett SA, Alfaro JF, Sáez FA, et al. Postharvest treatment of hydrogen sulfide delays the softening of Chilean strawberry fruit by downregulating the expression of key genes involved in pectin catabolism. Int J Mol Sci 2021;22(18):10008. https://doi.org/10.3390/ijms221810008 PMid: 34576171.
[47] Wang X, Lin L, Tang Y, et al. Transcriptomic insights into citrus segment membrane's cell wall components relating to fruit sensory texture. BMC Genomics 2018;19(1):280. https://doi.org/10.1186/s12864-018-4669-y PMid: 29685103.
[48] Yao S, Wang Z, Cao Q, et al. Molecular basis of postharvest granulation in orange fruit revealed by metabolite, transcriptome and methylome profiling. Postharvest Biol Technol 2020;166:111205. https://doi.org/10.1016/j.postharvbio.2020.111205.
[49] Zhong R, Lee C, Zhou J, et al. A battery of transcription factors involved in the regulation of secondary cell wall biosynthesis in *Arabidopsis*. Plant Cell 2008;20(10):2763–82. https://doi.org/10.1105/tpc.108.061325 PMid: 18952777.
[50] Napiroon T, Bacher M, Balslev H, et al. Scopoletin from *Lasianthus lucidus* Blume (Rubiaceae): a potential antimicrobial against multidrug-resistant *Pseudomonas aeruginosa*. J Appl Pharmaceut Sci 2018;8(9):1–6. https://doi.org/10.7324/JAPS.2018.8901.
[51] Lado J, Cronje P, Alquézar B, et al. Fruit shading enhances peel color, carotenes accumulation and chromoplast differentiation in red grapefruit. Physiol Plantarum 2015;154(4):469–84. https://doi.org/10.1111/ppl.12332. PMid: 25676857.
[52] Dautermann O, Lohr M. A functional zeaxanthin epoxidase from red algae shedding light on the evolution of light-harvesting carotenoids and the xanthophyll cycle in photosynthetic eukaryotes. Plant J 2017;92(5):879–91. https://doi.org/10.1111/tpj.13725. PMid: 28949044.
[53] Buaban P, Beckles DM, Mongkolporn O, et al. Lycopene accumulation in pummelo (*Citrus Maxima* [Burm.] Merr.) is influenced by growing temperature. Int J Fruit Sci 2020;20(2):149–63. https://doi.org/10.1080/15538362.2019.1605559.
[54] Khoo HE, Azlan A, Tang ST, et al. Anthocyanidins and anthocyanins: colored pigments as food, pharmaceutical ingredients, and the potential health benefits. Food Nut Res 2017;61(1):1361779. https://doi.org/10.1080/16546628.2017.1361779. PMid: 28970777.
[55] Fabroni S, Ballistreri G, Amenta M, et al. Anthocyanins in different *Citrus* species: an UHPLC-PDA-ESI/MS^n-assisted qualitative and quantitative investigation. J Sci Food & Agri 2016;96(14):4797–808. https://doi.org/10.1002/jsfa.7916. PMid: 27435016.
[56] Zhang H, Du C, Wang Y, et al. The *Reaumuria trigyna* leucoanthocyanidin dioxygenase (*RtLDOX*) gene complements anthocyanidin synthesis and increases the salt tolerance potential of a transgenic Arabidopsis *LDOX* mutant. Plant Physiol Biochem 2016;106:278–87. https://doi.org/10.1016/j.plaphy.2016.05.005. PMid: 27219053.